Optical Materials 84 (2018) 330–334

Contents lists available at ScienceDirect

Optical Materials

journal homepage: www.elsevier.com/locate/optmat

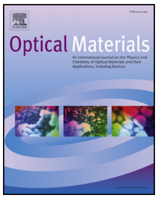

Fabrication and characterizations of $(Tb_{1-x}Pr_x)_3Al_5O_{12}$ magneto-optical ceramics for Faraday isolators

Qiang Liu[a], Xiaoying Li[a,b], Jiawei Dai[b], Zhaoxiang Yang[b], Tengfei Xie[b], Jiang Li[b,*]

[a] School of Material Science and Engineering, Jiangsu University, 301 Xuefu Road, Zhenjiang, 212013, China
[b] Key Laboratory of Transparent Opto-functional Inorganic Materials, Shanghai Institute of Ceramics, Chinese Academy of Sciences, Shanghai, 201899, China

ARTICLE INFO

Keywords:
$(Tb_{1-x}Pr_x)_3Al_5O_{12}$
Magneto-optical ceramics
Fabrication
Characterizations

ABSTRACT

Praseodymium doped terbium aluminum garnet (Pr:TAG) magneto-optical ceramics with different doping concentrations were fabricated by vacuum pre-sintering and hot isostatic pressing (HIP) post-treatment from the co-precipitated Pr:TAG nanopowders. It is found that all the as-synthesized powders exhibit a pure TAG phase and show good dispersity. The in-line transmittance of Pr:TAG ceramics fabricated by pre-sintering at 1700 °C for 20 h and HIP post-treating at 1700 °C for 3 h decreases from 80.6% to 76.3% at 1064 nm with the Pr^{3+} doping concentration increasing from 0 at% to 2.0 at%. The Verdet constant of the 2.0 at% Pr:TAG ceramics at 633 nm is -189.8 rad T^{-1} m^{-1}, which is 42% larger than that of the commercial TGG single crystals (-134 rad T^{-1} m^{-1}). The superior characteristics of the Pr:TAG ceramics indicate that they have great potential to meet the increasing requirements for magneto-optical devices used in the visible and near-infrared wavelength.

1. Introduction

With the development of optical communication technology, the laser source is required to possess characteristics such as high power, wide band, and high reliability. Damage caused by the back-reflections in the optical path has become a serious problem that must be primely solved. Therefore, Faraday isolator (FI) which can block the back-reflections has become an essential optical device used in the high-power lasers and advanced optical communication systems [1–3]. Currently, the most commonly used magneto-optical material in the visible and near-infrared range is terbium gallium garnet ($Tb_3Ga_5O_{12}$, TGG) single crystal due to its high Verdet constant and excellent optical quality [4,5]. In fact, terbium aluminum garnet ($Tb_3Al_5O_{12}$, TAG) has a higher Verdet constant than TGG, and it is thought to be a more promising magneto-optical material for the Faraday isolators of the next-generation [6–8]. However, it is very difficult to grow TAG single crystal because it melts incongruently with a crystallization of $TbAlO_3$ (TAP) phase [9]. Even though it can be grown by the floating zone (FZ) method or the micro-pulling-down method, the size of the as-grown TAG single crystals is too small, which is difficult to be applied for industrial applications [6,10,11].

TAG transparent ceramics can effectively avoid the incongruent melting problems since its fabrication temperature is lower than the melting point [12–15]. In addition, with the development of the transparent ceramic fabrication technology, TAG ceramics exhibit outstanding optical quality, good thermal properties and excellent magneto-optical properties [16–20]. Usually, TAG transparent ceramics can be fabricated by two main methods. One is solid-state reactive sintering of the commercial oxide powders, and the other one is vacuum sintering of the wet-chemical synthesized powders combined with hot isostatic pressing (HIP) post-treatment [21,22]. In 2011, Lin et al. firstly reported that the TAG transparent ceramics were prepared by the solid-state reaction and vacuum sintering technology. The in-line transmittance of the TAG ceramic is close to 70% in the 500–1500 nm region, and the Verdet constant is -172.7 rad T^{-1} m^{-1} at 632.8 nm, which is about 1.3 times as high as that of the commercial TGG single crystal [23]. Using the spray granulation powders, Ikesue successfully prepared the $(Tb_xY_{1-x})_3Al_5O_{12}$ ($x = 0.5$–1.0) transparent ceramics with ultralow optical loss, and the transmittance at 1064 nm of $(Tb_{0.6}Y_{0.4})_3Al_5O_{12}$ and TAG ceramics are 83.4% and 82.4%, respectively [24]. Dai et al. successfully fabricated highly transparent TAG ceramics using the co-precipitated nanopowders with tetraethoxysilane (TEOS) as sintering aids, and the in-line transmittance of the prepared TAG ceramic is about 80% in the wavelength range of 500–1300 nm [25].

Many works have demonstrated that the Verdet constant of the TAG transparent ceramics can be improved by adding dopants. For example, it has reported that TAG ceramics doped with Ce^{3+}, Si^{4+}, Ti^{3+} and

---

[*] Corresponding author.
E-mail address: lijiang@mail.sic.ac.cn (J. Li).

https://doi.org/10.1016/j.optmat.2018.07.028
Received 17 June 2018; Received in revised form 3 July 2018; Accepted 12 July 2018
0925-3467/

Ho^{3+} ions have higher values of Verdet constant than pure TAG ceramics [13,26–28]. The enhancement of the Verdet constant can be attributed to the quantum based super-exchange interaction between Tb^{3+} and other paramagnetic RE^{3+} ions [29]. Recently, Chen et al. have demonstrated that Pr^{3+} doped TGG single crystal possesses a higher Verdet constant than that of the pure TGG single crystal [30], indicating that Pr^{3+} doping can also improve the Verdet constant of the Faraday material.

In this work, we synthesized Pr:TAG nanopowders with different doping concentrations by a co-precipitation method. The influence of Pr^{3+} doping concentration on the phase composition and morphology of the as-synthesized powders was investigated. Subsequently, Pr:TAG transparent ceramics were fabricated by vacuum sintering followed by HIP post-treatment. The optical quality, microstructure, and magneto-optical property of the Pr:TAG ceramics were also systematically studied.

2. Experimental

$Tb(NO_3)_3$ and $Pr(NO_3)_3$ solutions were prepared by dissolving Tb_4O_7 (99.99%, Yuelong New Materials Co., Ltd., Shanghai, China) and Pr_6O_{11} (99.99%, Changting Jinlong New Materials Co., Ltd., Fujian, China) in the hot high-purity nitric acid. Nitrate solution of Al^{3+} was obtained by dissolving $Al(NO_3)_3{\cdot}9H_2O$ (99.0%, Sinopharm Chemical Reagent Co., Ltd.) in deionized water under stirring. According to the chemical formula of $(Tb_{1\text{-}x}Pr_x)_3Al_5O_{12}$, different metal solutions were mixed until the volume of the solution was 500 mL, and the concentration of Al^{3+} in the solution was 0.3 M. Ammonium hydrogen carbonate (Analytical grade, Aladdin, AHC) was dissolved in deionized water as the precipitant solution and the concentration of AHC solution was set as 1.5 M. Ammonium sulfate (99.0%, Sinopharm Chemical Reagent Co., Ltd.) was added as dispersant. For better cation homogeneity, the reverse-strike technique was selected to prepare precursors. 500 mL of the nitrate solution was added to 640 mL of the precipitant solution under mild agitation at a dripping speed of about 20 mL/min. The resultant suspension was aged for 1 h at room temperature without stirring, and then it was filtered and washed four times using distilled water and twice using ethanol to remove the by-products. After drying at 70 °C for 36 h, the dried precursors were sieved through 200-meshs screen and then calcined at 1100 °C for 4 h to obtain the Pr:TAG nanopowders. The resultant powders with 0.5 wt% TEOS (> 99.999%, Alfa Aesar, Tianjin, China) as sintering aid were ball-milled in ethanol for 12 h. After ball milling, the slurry was dried at 70 °C for 2 h, sieved through a 200-mesh screen and then calcined at 600 °C for 4 h to remove organic ingredients. The obtained powders were then dry-pressed into pellets and further cold isostatic pressing (CIP) at 250 MPa. The samples were vacuum sintered at 1700 °C for 20 h combined with HIP post-treatment at 1700 °C for 3 h under 200 MPa in Ar atmosphere.

The phases of the nanopowders were analyzed by the X-ray diffractometry in the 2θ range of 10–80° using nickel-filtered Cu K_α radiation. (XRD, Mode-l D/max2200 PC, Rigaku, Japan). The morphologies of powders and the microstructures of the ceramic surfaces were performed by a field emission scanning electron microscopy (FESEM, S-8220, Hitachi, Japan). Grain sizes of the ceramic samples were calculated by the linear intercept method. Specific surface areas of the powders were investigated by Norcross ASAP 2010 micromeritics with N_2 as the absorption gas at 77 K. The in-line transmittance of the both-side polished Pr:TAG transparent ceramics was characterized by a UV-VIS-NIR Spectrophotometer (Model Cary-5000, Varian, USA) in the wavelength range of 300–1800 nm at room temperature. The Verdet constant was measured by the extinction method with an instrument consisting of a He–Ne laser, an electromagnet and two polarizers. The measurement was carried out at room temperature, the applied magnetic field is 1.18 T, and the thickness of the sample is 1.2 mm.

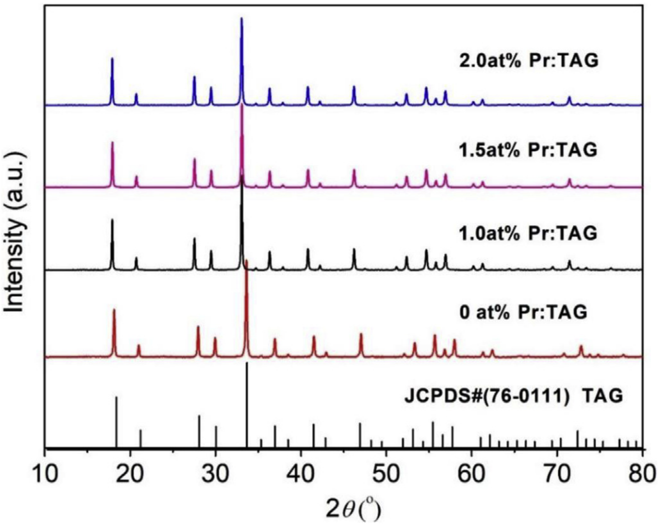

Fig. 1. XRD patterns of the $(Tb_{1\text{-}x}Pr_x)_3Al_5O_{12}$ powders (x = 0, 0.01, 0.015, 0.02).

3. Results and discussion

The XRD patterns of the Pr:TAG powders with different doping concentrations obtained by calcining the precursors at 1100 °C for 4 h are shown in Fig. 1. It can be seen that diffraction peaks of all the powders are consistent with the cubic structure of TAG (JCPDS 76–0111). Pr^{3+} ions in the TAG lattice mainly occupy the Tb^{3+} sites instead of the Al^{3+} sites. The lattice parameters of the Pr:TAG powders are slightly larger than that of the pure TAG powders because the ionic radius of Pr^{3+} (0.1013 nm) is larger than that of the Tb^{3+} (0.0923 nm), and the lattice parameters of the Pr:TAG powders with doping concentrations of 0 at%, 1.0 at%, 1.5 at%, and 2.0 at% are 12.0826, 12.0926, 12.0930 and 12.0955 Å, respectively.

Fig. 2 shows the FESEM micrographs of the Pr:TAG powders with different doping concentrations. It is found that all the powders exhibit good homogeneity and dispersity, which is beneficial to the fabrication of transparent ceramics with excellent optical quality. The specific surface areas of Pr:TAG powders with Pr^{3+} concentrations of 0 at%, 1.0 at%, 1.5 at%, and 2.0 at% are 10.8, 10.3, 11.1, and 10.4 m^2/g, respectively. It indicates that the doping concentration of Pr^{3+} has little impact on the morphology and dispersity of the powders.

Fig. 3 shows the photograph of the Pr:TAG ceramics (1.2 mm thick) with different doping concentrations prepared by vacuum sintering at 1700 °C for 20 h and HIP post-treatment at 1700 °C for 3 h under 200 MPa. As can be seen, all the Pr:TAG ceramics exhibit good optical properties as the letters under them can be seen clearly. All the Pr:TAG ceramics are slightly green in color because of the absorption of Pr^{3+} ions in the visible light band, and the color of the ceramic samples deepens with increasing the Pr^{3+} doping concentration.

The in-line transmission curves of the Pr:TAG transparent ceramics (1.2 mm thick) with different doping concentrations are shown in Fig. 4. It can be seen that the pure TAG ceramic shows the best transparency, and the transmittance is about 80% in the 800–1500 nm region. The optical transmittance of the ceramic samples decrease slightly with the Pr^{3+} doping concentration increasing from 0 at% to 1.0 at%, 1.5 at% and 2.0 at%, and the in-line transmittances of Pr:TAG transparent ceramics at 1064 nm are 80.6%, 79.3%, 78.3% and 76.3%, respectively. It indicates that as the Pr^{3+} doping concentration increases, more optical scattering centers lead to a decrease in the transmittance of the samples, as can be confirmed in Fig. 5. There are some absorption bands located at around 453, 475, 488,609, 1029 and 1526 nm, which correspond to the transitions of Pr^{3+} ions from the ground state $^3H_4$ to excited state $^3P_2$, $^3P_1+{}^1I_6$, $^3P_0$, $^1D_2$, $^1G_4$ and $^3F_3+{}^3F_4$, respectively. The